Available online at www.sciencedirect.com

SciVerse ScienceDirect

Ceramics International 39 (2013) 4539–4549

CERAMICS INTERNATIONAL

www.elsevier.com/locate/ceramint

Synthesis of nanocrystalline hydroxyapatite by precipitation using hen's eggshell

D.L. Goloshchapov, V.M. Kashkarov, N.A. Rumyantseva, P.V. Seredin*, A.S. Lenshin, B.L. Agapov, E.P. Domashevskaya

Voronezh State University, Universitetskaya sq. 1, 394006 Voronezh, Russian Federation

Received 2 October 2012; received in revised form 20 November 2012; accepted 20 November 2012
Available online 27 November 2012

Abstract

Hydroxyapatite (HAP) is a substance that is most actively used in orthopedia and dentistry as a biocoating of implants in order to improve its osteointegration with bone tissue. HAP was synthesized by precipitation technique with the use of the biological source — hen's eggshell. X-ray diffraction (XRD) investigations, IR-spectroscopy, scanning electron microscopy (SEM) demonstrate that the obtained powder-like material in the form of globules from 4 to 5 μm in size is single-phase, thermally stable up to 900 °C and morphologically uniform. The globules consist of nanocrystals with the average size of about 30 nm.

Keywords: Hydroxyapatite; Biomaterials; Characterization; X-ray; diffraction

1. Introduction

The study of the bone tissue formation and growth on the implants surface used to recover the functions of a human and animal bone [1,2], as well as stomatologic investigations of cementation processes and formation of filler — dental enamel — dentin bond [3] affirm the necessity in new materials close to biogenic composites in their structure, "architecture" and chemical composition which could improve such characteristics as adhesion, bioactivity and biocompatibility [4]. These biomaterial properties depend on a number of factors. And they, in turn, are determined by the choice of reagents and parameters of synthesis as well as a need to correspond by all parameters with human bone tissue. A crystal-chemical analog of the bone tissue mineral component is hydroxyapatite (HAP – $Ca_{10}(PO_4)_6(OH)_2$) [5]. The presence of this biomineral in natural structures in nanocrystalline state (~5–10 nm) is the result of osteogenesis and it facilitates the natural calcium exchange in an organism, thus affecting all the interactions involving this compound [6].

Applicability of biomaterials obtained in laboratory conditions is determined by such characteristics of the samples as their structure, composition and crystallinity: all these parameters depend on specific parameters of synthesis [7,8]. Hydroxyapatite in the nanocrystalline form is usually applied for implant coatings, dental cements and dental toothpastes due to a high bioactivity of this compound and a possibility of creating composite materials based on this compound [9].

Nanocrystalline HAP can be synthesized using different technologies. Among them are solid-phase synthesis and the wet-chemistry methods. Solid-phase synthesis techniques include reactions with the participation of solid precursor, transformed into HAP by different kinds of actions and the mechanical activation methods.

HAP production involving solid-state reactions that proceed between ($Ca(NO_3)_2 \cdot 4H_2O$) and ($Na_3PO_4 \cdot 12H_2O$) along with grinding, stirring and heating under microwave irradiation makes it possible to synthesize high-purity substance, which is morphologically uniform and contains elongated ellipsoidal particles with almost similar narrow spread in diameter. The difference in technological modes (time of exposure to radiation) has a strong effect on morphology of the samples. Size of the particles reaches 60–400 nm [10].

*Corresponding author. Tel.: +74732208363.
E-mail addresses: ftt@phys.vsu.ru, paul@phys.vsu.ru (P.V. Seredin).

0272-8842/$ - see front matter © 2012 Elsevier Ltd and Techna Group S.r.l. All rights reserved.
http://dx.doi.org/10.1016/j.ceramint.2012.11.050

The mechanical activation method based on the use of planetary ball mills does not require microwave radiation. In this method hydroxides and calcium salts are used as precursors, as well as alkali metal salts. Mechanic–chemical synthesis performed in the solid-state phase is accompanied by water formation caused by redox interaction between precursors. H_2O participates in the process of interaction between the obtained components facilitating the end products formation under lower mechanical loads. For example, $Ca_2(H_2PO_4)_2H_2O$, CaO and $SiO_2 \cdot 0.59H_2O$ were used to obtain hydroxyapatite with silicon inclusion ($Ca_{10}(PO_4)_{4.28}(SiO_4)_{1.72}(OH)_{0.28}$). The produced materials satisfy the established requirements concerning purity, phase composition and physico–chemical properties [11].

The wet-chemistry methods applied for HAP production use sol–gel technology, spray pyrolysis technique, hydrothermal method and precipitation. Sol–gel technology allows to obtain well-crystallized materials with the particle size from 10 to 100 nm that are stable up to 1200 °C [12,13].

Thermal heating of the reaction mixture of calcium- and phosphorus-containing components in the hydrothermal synthesis methods provides well-crystallized samples with a high temperature stability [14]. Thus it is possible to obtain materials with nanocrystals of ~45–65 nm in size.

Precipitation methods based on titration of solutions containing the reagents under specified rate allow to produce crystallites of less size in similar conditions. Due to this fact the above-mentioned methods are most actively used for obtaining of nanocrystalline hydroxyapatite samples [15,16]. Orthophosphoric acid salts and various calcium sources ($CaCO_3$, $Ca(NO_3)_2$, $CaCl_2$) [17] can be chosen as initial substances in these processes. The technique makes it possible to synthesize materials that are different in composition, stoichiometry and crystallinity taking into account technological modes and ambient conditions.

In Ref. [18] using both deposition with applying of the raw materials $Ca(NO_3)_2 \cdot 4H_2O$, $(NH_4)_2HPO_4$ and NH_4OH with subsequent drying for 72 h. the samples were synthesized and then annealed at 800 °C for 1 h. The obtained HAP corresponded to the stoichiometric ratio of Ca/P=1.66, while the conducted morphological investigations demonstrated that the crystallites were of 0.55–1.2 μm in diameter and 2.3–2.9 μm in length. Materials with similar substructure are applied in medicine as fillers for bone defects, as well as for acceleration of bone tissue regeneration, in dental pastes for enhancing cement adhesion.

The processes assuming low-temperature treatment of precipitate during semi-continuous synthesis by means of solutions ($CaCl_2$ (3 · 06 M)) and (K_2HPO_4 (0 · 38 M)), make it possible to obtain nanocrystalline materials with crystallite size of 60–90 nm and 60–200 nm. Precipitation technique provides obtaining of morphologically uniform samples in the presence of tetrahydrate of calcium nitrate and ammonium phosphate in a mixed solution [19]. The produced material is identified as HAP with morphologically uniform structure in the form of needle-like spikes with a length up to 100 nm.

Synthesis of nanocrystalline samples can be performed with the use of calcium hydroxide ($Ca(OH)_2$) and orthophosphoric acid (H_3PO_4) in specially selected modes and for certain concentrations of reacting compounds [20]. Moreover, the interaction between different phosphate- and calcium-containing mixtures at the given rates of mixing and titration as well as temperature modes and concentration values allows to obtain materials with morphological features similar to those ones in biogenic materials [21]. So, precipitation process with long-term synthesis gives the possibility to influence on the formation of hydroxyapatite in different ways: either by changing precipitate temperature [22], or by exposure of the reaction area to microwave irradiation [23]. The produced materials demonstrate submicrocrystalline structure (crystallite size about ~53–87 nm or ~100 nm, respectively).

Nanocrystalline hydroxyapatite samples can be synthesized by precipitation using natural calcium sources thus simplifying technological process of the material production. In Refs. [24,25] nanocrystallie HAP was obtained with the use of bird's eggshell. The proposed idea is based on the fact that eggshell mainly consists of calcium carbonate ($CaCO_3$) that is dissociated at the temperature above 900 °C into carbon dioxide (CO_2) and calcium oxide (CaO). The latter is used either for producing calcium hydroxide titrated with orthophosphoric acid solution in order to obtain HAP, or is mixed with $(NH4)_2HPO_4$, resulting in HAP formation as the end product with definite morphology and nanocrystals of different size in the range from 10 to 100 nm.

Production of various implants for orthopedic surgery involves several methods of HAP deposition onto Ti, TiO_2 and other substrates, for example, ion-plasma, magnetron, hydrothermal, electrochemical and some others [8]. Consequently, the temperature behavior of HAP in different processes is very important. Pure hydroxyapatite is stable up to 1200 °C [5], and then, according to XRD data, high-temperature form of tri-calcium phosphate α-$Ca_3(PO_4)_2$ (α-TCaPh) appears. The influence of impurities and composition inhomogeneity depending on the synthesis method reduces the temperature stability and HAP decomposition can be observed already at 900 °C [12,22]. At the same time, the interval of working temperatures in the coating deposition process (300–400 °C) allows applying HAP with the lower temperature stability as compared with pure hydroxyapatite. Besides, the features of phase transitions into carbonate-substituted hydroxyapatite can be also observed if HAP is synthesized in the atmosphere due to the presence of CO_2. In different technological methods (by annealing, choosing synthesis parameters — for example, pH) it is possible to escape CO_3^{2-} inclusion into crystal lattice or recrystallize carbonate-substituted HAP into pure HAP [26]. In this case the most convenient way to control the obtained material is the application of IR-spectroscopy which can detect vibration modes of CO_3^{2-} inclusions at very low concentrations [27].

It should be noted that for various processes of hydroxyapatite synthesis the concentration of initial reagents is chosen in such a way that Ca/P ratio should be equal to the stoichiometric one 1.67 since in the mineral component of bone tissue Ca/P ratio is close to the given value and can vary from 1.5 to 1.9 [5]. Moreover, according to the results of a number of works HAP samples with Ca/P ratio = 1.67 are more stable relative to thermal exposure and solubility in weak acids. Ceramics based on these kinds of materials demonstrated the best characteristics in mechanical properties, density, hardness and some others [28].

The purpose of this work is to find the optimal parameters of nanocrystalline HAP synthesis obtained by precipitation with the use of bird's eggshell as the calcium source, as well as to study of the properties and characteristics of the synthesized samples.

1.1. Technology of Samples synthesis and methods of investigations

Precipitation technique is the basis of the elaborated HAP preparation technology. A special feature of our method is producing the initial component for a chemical reaction — calcium oxide (CaO) by treating the bird's eggshell. Eggshell is chosen as source since it consists of 95% calcite — $CaCO_3$. The rest of it comprises an organic component, i.e. several layers of interlaced protein fibers, as well as various mineral salts ($<1\%$) arranged on the protein fibers just as calcite. Under heating $CaCO_3$ is dissociated to yield CaO and CO_2:

$$CaCO_3 \rightarrow CaO + CO_2 (T = 900\ ^\circ C) \quad (1)$$

During anneal the organic component of eggshell is burnt out and the residue contains CaO with low ($\leq 1\%$) content of impurities.

Nanocrystalline HAP synthesis involves step-by-step precipitate preparation. Preliminarily the eggshell containing $CaCO_3$ was thoroughly washed and then annealed for 2 h. at 900 °C according to Eq. (1). After that the obtained calcium oxide was immediately (at ~100 °C) mixed with distilled water and the mixture was left until complete cooling:

$$CaO + H_2O \rightarrow Ca(OH)_2 + Q \quad (2)$$

where Q is a heat released in the reaction.

The obtained calcium hydroxide $Ca(OH)_2$ was titrated with a solution of orthophosphoric acid H_3PO_4 (0,6 M) at the room temperature for producing of hydroxyapatite

$$10Ca(OH)_2 + 6H_3PO_4 \rightarrow Ca_{10}(PO_4)(OH)_2 + 18H_2O \quad (3)$$

The synthesis process was controlled by measuring pH in the reaction (pH-meter Checker 1 HI 98130, HANNA) with an increment 0.5 within the range of 9 to 7 as well as by the rate of acid addition to the precipitate.

To conduct various kinds of analysis HAP samples were dried at 400 °C for 1 h. It should be noted that all the process of hydroxyapatite preparation requires different time which depends on the initial components concentration, and the process itself does not need any special conditions. In our experiments the end product (powder-like HAP) was ready after 36 h.

Investigations of the obtained HAP samples characteristics were performed using a set of structural and spectral methods of analysis. For example, the study of impurities in the initial eggshell involved XRD analysis and X-ray spectral microanalysis (MA). According to the XRD and MA data the concentrations of such metals as Fe, Zn, Cu, Sr, Mn in the eggshell and obtained samples were no more than 0.0001%.

XRD technique was applied to study the structural characteristics of the samples synthesized at different pH values. The final purpose of the study was to determine the phase composition and the range of temperature stability for the obtained materials. X-ray diffractograms were obtained with the diffractometer DRON-4 07 and X-ray tube with cobalt anode (Co $K_{\alpha 1,2}$ emission, $\lambda = 1.7903$ Å).

The fine structure properties, vibration groups, the type of atomic bonds in the obtained materials, their changes depending on the samples treatment were determined and analyzed by means of IR Fourier spectroscopy (FTIR). IR spectra were obtained with the FTIR spectrometer VERTEX V-70, BRUKER by attenuated total internal reflection (ATR). The spectral range involved an interval from 550 to 4000 cm^{-1}.

Specific surface which is connected with such characteristics of materials and nanostructures as catalytic activity, electrostatic properties, light scattering, ability of agglomeration, water retention, duration of storage [29], was determined with SORBI-MS unit. This unit compares the volumes of gas adsorbed by the sample under investigation with that one adsorbed by the reference sample with the known specific surface. Nitrogen was used as gas adsorbate. To measure the adsorbed gas volume thermal desorption technique was applied. The measurements were performed at four different partial relative values of pressure of the adsorbed gas. Calculations of the specific surface were based on the Brunnauer–Emmet–Teller (BET) theory [29].

Scanning electron microscopy (SEM) was applied to determine of morphological features of the obtained samples with the scanning electron microscope JSM-6380LV (JEOL). Thin gold layer was deposited on the samples before conducting SEM investigations in order to reduce charging effects due to dielectric nature of HAP. Besides, we have made microanalysis of the samples with the use of the energy-dispersion attachment Inca-250 to the electron microscope. This allowed us to find that with the help of this synthesis method it is possible to obtain HAP with different Ca/P ratio.

2. Results of investigations

2.1. XRD analysis of synthesized HAP

The phase composition for the investigated HAP samples was determined by comparison of the XRD analysis results for the investigated samples with the JCPDS-ICDD data [30]. Table 1 represents the interplanar spacing values and relative intensities for the diffraction lines in synthesized

Table 1
Interplanar spaces and relative intensity of synthesized material, polycrystalline HAP and ICDD data.

HAP ICDD 2007 No. 01-074-0565			Poly. HAP		HAP 400 °C		HAP 700 °C		HAP 900 °C		Whitlockite ICDD No. 00-055-0898		
d, (Å)	*I*	hkl	*d*, (Å)	*I*	*d*, (Å)	*I*	*d*, (Å)	*I*	*d*, (Å)	*I*	*d*, (Å)	*I*	hkl
8.17	12	**100**	8.12	0.9			8.22	3.84	8.10	10.32	8.13	9	**012**
											6.48	16	**104**
5.26	6	**101**	5.28	0.7			5.31	5.75	5.18	14.33	5.18	22	**110**
4.07	10	**200**	4.11	8.1	4.11	36	4.09	4.66	4.06	10.03	4.06	11	**024**
3.89	10	**111**	3.88	1.8			3.88	6.3	3.88	5.16			
3.51	2	**201**	3.74	0.6							3.46	26	**1010**
3.44	40	**002**	3.43	34	3.41	46.1	3.45	32.05	3.44	44.41	3.36	9	**122**
3.17	12	**102**	3.18	5.8	3.15	10.9	3.19	7.67	3.19	30.37	3.21	53	**214**
3.08	18	**210**	3.08	14	3.07	10.9	3.09	15.62	3.08	11.75	3.01	12	**300**
											2.88	100	**0210**
2.81	100	**211**	2.81	100	2.83	100	2.81	100	2.81	100			
2.78	60	**112**	2.77	60	2.77	97.5	2.77	60	2.78	49.28	2.76	22	**128**
2.72	60	**300**	2.71	62	2.72	56	2.72	63.29	2.72	57.31	2.72	7	**036**
2.63	25	**202**	2.62	23	2.64	22.6	2.64	21.92	2.63	21.78	2.61	65	**220**
2.53	6	**301**	2.52	3.3	2.52	4.31	2.53	6.03	2.54	3.72	2.52	13	**2110**
2.30	8	**212**	2.29	6.6					2.30	6.59	2.41	8	**226**
2.26	20	**130**	2.26	22	2.26	16.9	2.26	24.38	2.26	23.5	2.37	6	**315**
2.23	2	**221**							2.23	3.72	2.26	6	**1016**
2.15	10	**131**	2.15	6.7			2.15	7.4	2.15	9.74	2.19	13	**404**
2.13	4	**302**									2.16	11	**3012**
2.06	8	**113**	2.06	4	2.05	4.5	2.06	6.03	2.06	8.88	2.03	10	**048**
2.00	6	**203**	2.00	4.1					2.00	6.59	2.00	8	**2212**
1.94	30	**222**	1.94	30	1.94	20.9	1.95	27.4	1.94	32.09	1.93	30	**327**
1.89	16	**132**	1.89	13	1.88	12.7	1.89	13.42	1.89	21.78	1.89	18	**238**
1.87	6	**230**							1.87	12.61	1.87	15	**416**
1.84	40	**213**	1.84	34	1.83	29.4	1.84	30.96	1.84	36.68			
1.80	20	**321**	1.80	17	1.80	12.5	1.80	16.16	1.81	18.05			
1.78	12	**140**	1.78	12			1.78	12.9	1.78	13.47			
1.75	16	**402**	1.75	12	1.76	11.7	1.76	10.96	1.75	10.6			
1.72	20	**004**	1.72	17	1.72	13.3	1.72	12.05	1.72	32.09	1.72	34	**2020**
1.68	4	**104**									1.68	8	**508**
1.64	10	**322**	1.64	5.8			1.64	7.12	1.64	6.59			
1.61	8	**313**	1.61	3.3									
1.59	4	**501**									1.60	6	**339**
1.54	6	**240**	1.54	3.6					1.54	11.17	1.55	9	**1410**
1.53	6	**331**	1.53	2.7							1.54	7	**3216**
1.50	10	**124**	1.50	6.4					1.50	7.16			
1.47	12	**502**			1.47	8.06			1.47	9.46			
1.46	4	**510**											
1.452	13	**304**			1.45	10.3			1.45	12.32			

samples annealed at 400 °C, 700 °C and 900 °C, along with the data of International Center of Diffraction Data (ICDD).

As one can see from the comparison of the interplanar spacings and intensities (Table 1), the synthesized material proved to be hydroxyapatite. XRD data analysis for the samples exposed to anneal at different temperatures demonstrated that the powder samples obtained from precipitate with the value of pH = 8.5 remain single-phase HAP up to the temperature of anneal below 900^0C. In the samples annealed at 900 °C, diffraction lines appear that are related to calcium diphosphate – whitlockite, and it means HAP decomposition (see Table 1).

In order to determine the size of the synthesized HAP crystallites we used the reference stoichiometric sample of microcrystalline hydroxyapatite obtained by standard technology [31] not using eggshell.

It is important that XRD patterns of the synthesized HAP samples annealed at 400 °C do not contain extra reflections and are characterized by low intensive and mostly broad lines as compared with the microcrystalline HAP (curves 2, 3 in Fig. 1). The crystallite size in the obtained material was estimated by the broadening of X-ray diffraction lines as compared with the microcrystalline sample. This analysis was made for reflection (002) in accordance with Scherer formula:

$$L = k\lambda/\beta\cos\theta \quad (4)$$

where L is a mean value of the crystallites size, k is a constant close to 1, λ is the X-ray emission wavelength

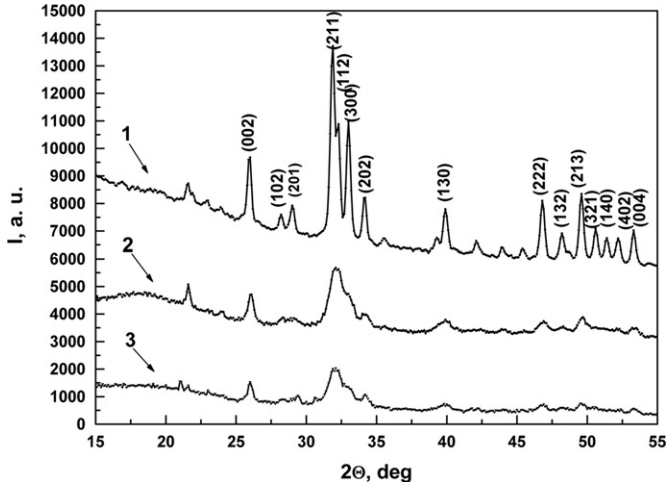

Fig. 1. Polycrystalline HAP (1) and samples of synthesized HAP (2 and 3). (Cu Kα radiation).

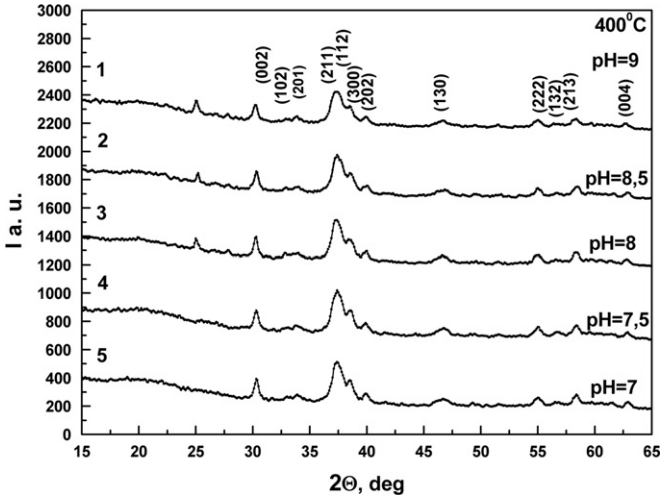

Fig. 2. Diffraction pattern of synthesized HAP with pH=9, 8.5, 8, 7.5, 7 annealed at 400 °C.

(Co $K_{\alpha 1,2}$; 1.7903 Å), β is X-ray reflection broadening, $\beta = \left(B^2 - b^2\right)^{1/2}$, where B — half-width of the diffraction line (002); b — half-width of the diffraction line (002) for the reference polycrystalline sample, θ — Bragg's angle of the diffraction line (002).

The estimated mean value for the crystallite size in the synthesized HAP according to Eq. (4) was 35 nm that agrees well with the results for HAP synthesized in a similar way in [20] ~30 nm, and also for the HAP in bone tissue: ~15 nm [24,25].

2.2. Influence of pH solution on the phase composition of hap annealed at different temperatures

XRD data for the samples obtained at different pH values in the range from 9 to 7 and annealed after the synthesis at 400 °C are presented in Fig. 2. Comparison of diffractograms does not show any differences for the samples synthesized at different values of pH in a solution that means the same phase composition of the nanocrystalline HAP samples.

The differences in characteristics of the material synthesized at different values of pH in solution — 9, 8.5, 8, 7.5, 7 become observable after anneal at 700 °C. Diffractograms presented in Fig. 3 show the following regularity: for the powder samples obtained from precipitates with less pH value of solutions — 7.5 and 7, i.e. for the higher concentration of acid (H_3PO_4), during the HAP synthesis one can see the beginning of hydroxyapatite decomposition with formation of whitlockite. The samples synthesized at pH values of the end solution equal to 9; 8.5; 8 at the temperature of 700 °C comprise a single phase — hydroxyapatite.

Comparison of the materials obtained at different pH values and annealed at 900 °C confirmed the idea: hydroxyapatite samples synthesized at the less values of pH for the end product precipitate (7.5 and 7) are completely transformed to whitlockite at the temperature of anneal while those ones with a greater pH value (9, 8.5, 8) keep

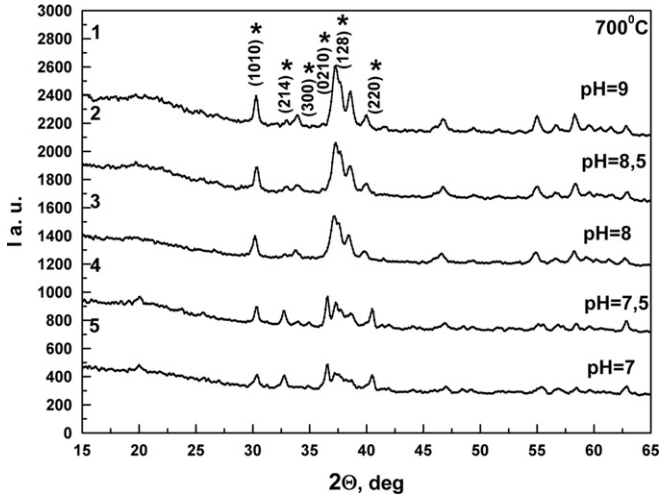

Fig. 3. Diffraction pattern of synthesized HAP with pH=9, 8.5, 8, 7.5, 7 annealed at 700 °C.

the phase of HAP simultaneously with the whitlockite phase that is observed in more or less amount in the samples annealed at 900 °C (Fig. 4).

Thus, the XRD analysis of the HAP samples synthesized at different pH values allows to make a conclusion that the nanocrystalline HAP samples obtained from precipitate with final pH=8.5 show the best temperature stability.

2.3. Infrared spectroscopy

Infrared vibration spectroscopy was applied to determine the qualitative composition of the synthesized material and to study the crystal lattice properties of hydroxyapatite.

Scientific works review provided information on the main vibration modes c of HAP. Therefore, with the help of IR spectroscopy it is possible to determine the presence

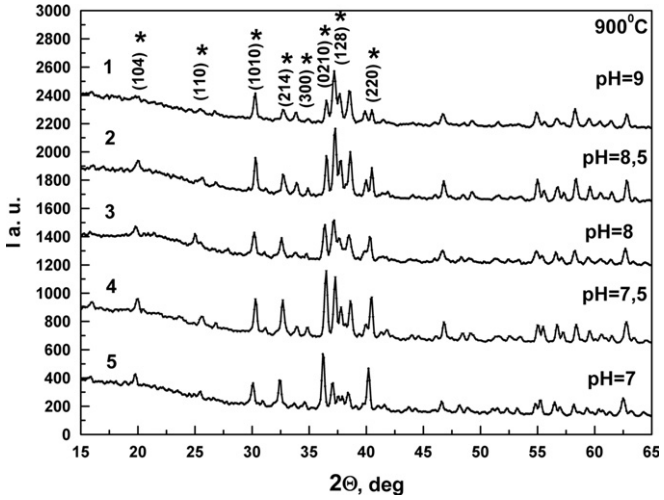

Fig. 4. Diffraction pattern of synthesized HAP with pH=9, 8.5, 8, 7.5, 7 annealed at 900 °C.

of characteristic bonds and groups of bonds in the synthesized material. The frequencies of vibration modes for certain bonds in the obtained HAP including those ones after anneal at different temperatures are given in Table 2 along with the data from the other references.

The analysis of the experimental data and those presented in literature demonstrated that the main vibration modes inherent to the crystalline HAP are also observed in the synthesized material. Moreover, in IR spectra of the synthesized HAP the peaks at 879 cm^{-1} and 1415 cm^{-1} with rather low intensity are observed which can be related with the group of CO_3 (Fig. 5). Their appearance can be caused by a high activity of the initial component CaO and the presence of CO_2 in the atmosphere during the synthesis process.

Figs. 6–8 represent IR spectra of the HAP samples synthesized at different pH values varying from 7 to 9. The HAP spectra obtained at different pH values with the subsequent anneal at 400 °C are presented in Fig. 6. All of them are related to a single phase — hydroxyapatite, according to the XRD data. As it is shown in Fig. 6, IR spectra of these samples do not involve any additional vibration modes as well, and it means the presence of only single phase — HAP in these samples.

Some features observed in IR spectra of the materials annealed at 700 °C involve the fine structure appearing in the vibration modes characteristic of phosphorus–oxygen group PO_4 for the HAP samples obtained from the solutions with pH values of 7 and 7,5. According to Fig. 7 additional peaks appear in IR spectra of these samples at 1114 cm^{-1}, 977 cm^{-1} and 948 cm^{-1}. It means that the second phase appears — whitlockite in accordance with the XRD data.

Appearance of whitlockite in the synthesized materials annealed at 700 °C means less temperature stability of these HAP samples as compared with the materials obtained at pH=8; 8.5; 9. As for the samples annealed at 900 °C (Fig. 8) the results of IR spectroscopy show that

Table 2
IR vibration modes of synthesized HAP and References [1–3].

Vibration line of characteristic groups	Vibration modes ν (cm^{-1})					
	Experimental data			References		
	400 °C	700 °C	900 °C	HAP[32]	HAP [33]	HAP [24]
PO_4 ν^4	573	573	573	564	574	571
PO_4 ν^4	602	601	598	610	601	607
OH	627	630	630	650	631	635
CO_3 (ν^3)	879	878	–	–	875	875
PO_4 (whitlockite)	–	–	949	–	–	–
PO_4 ν^1	963	963	962	962	962	961
PO_4 (whitlockite)	–	–	977	–	–	–
PO_4 ν^3	1022	1021	1017	1029	1040	1050
PO_4 ν^3	1090	1089	1087	1092	1090	1090
PO_4 (whitlockite)	–	–	1122	–	–	–
CO_3 (ν^3)	1415	1460	–	–	1410	1429
PO_4 (whitlockite)	1451	1456	–	–	1450	1460
OH	3570	3571	3573	3567	3572	3572

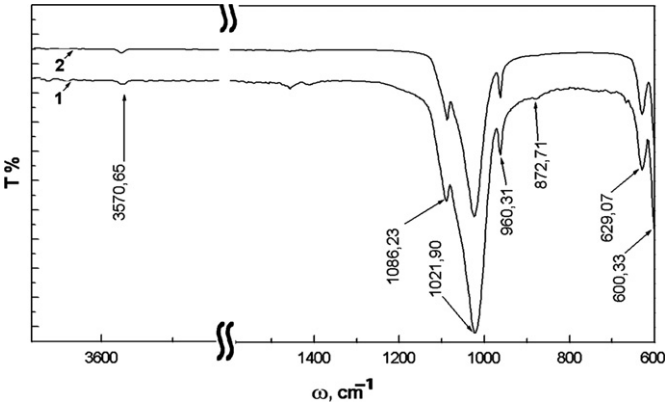

Fig. 5. Comparison of nanocrystalline (1) and polycrystalline (2) HAP.

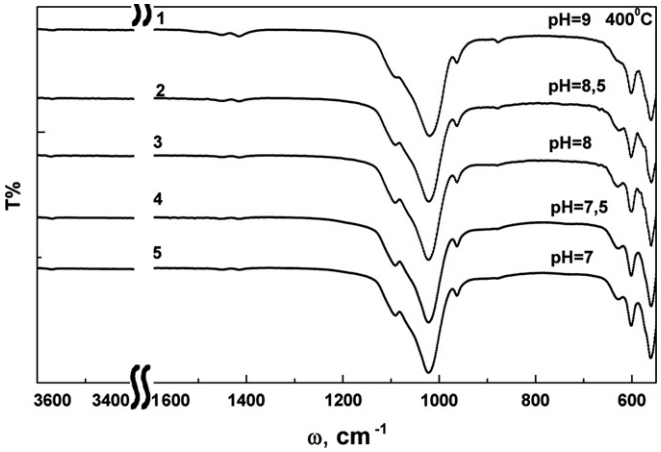

Fig. 6. IR spectra of HAP samples annealed at 400 °C.

the fine structure of vibration line characteristic of the phosphorus–oxygen group observed as additional peaks at 1114 cm^{-1}, 977 cm^{-1} and 948 cm^{-1} means the presence of the whitlockite phase that can be seen for all of the samples. This is in agreement with the XRD data. It should be also noted that in IR transmission spectra of a number of the HAP samples (Fig. 9) vibration modes localized at 1450 cm^{-1} and 1429 cm^{-1} can be observed. We relate these modes to CO_3^{2-} group. This substitution in the crystal lattice of HAP is characteristic for the material obtained by precipitation in the air.

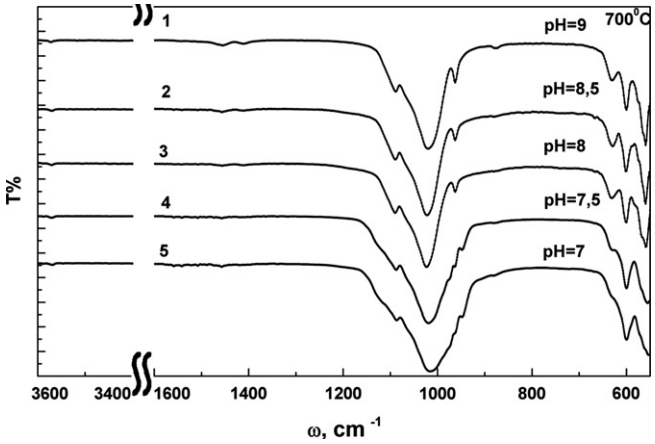

Fig. 7. IR spectra of HAP samples annealed at 700 °C.

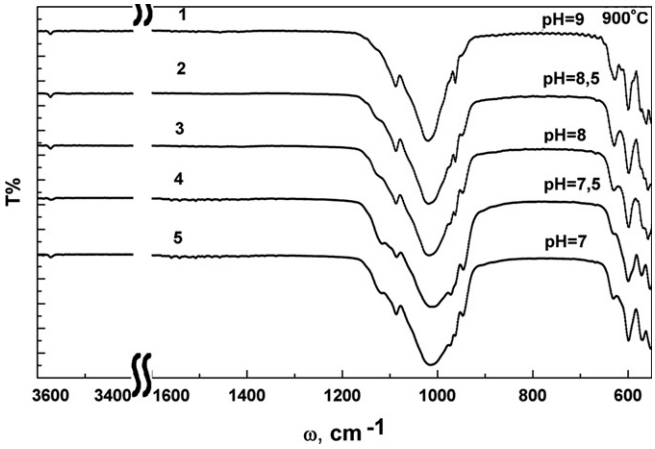

Fig. 8. IR spectra of HAP samples annealed at 900 °C.

A high activity of the initial component CaO and the presence of CO_2 in the process of synthesis can explain the presence of weak peaks at 879 cm^{-1}, 1429 cm^{-1} and 1450 cm^{-1}, characteristic of CO_3^{2-} group. These vibration modes characterize formation of carbonate-substituted hydroxyapatite of B-type that is in agreement with the data of [34]. It is also known that during phase transformations under high temperatures in HAP CO_3^{-2} is eliminated from the structure of hydroxyapatite. This fact is confirmed by IR spectra of the annealed samples (Fig. 9b). Besides this, the presence of carbonate ions depends on pH value during the HAP synthesis [35] and its content is reduced with a decrease of pH value that is illustrated in Fig. 9a.

It should be noted that inclusion of carbonate ion in the HAP structure does not change the hydroxyapatite phase composition and is not observed in X-ray diffraction. At the same time IR-spectroscopy is one of the most efficient method for detecting similar impurities in hydroxyapatites obtained in different technological conditions.

2.4. Thermal desorption of nitrogen

Specific area surfaces for HAP powders were calculated and the size of the powder particles was determined by measuring the volume of the gas adsorbed on the sample at four different partial pressure values (Fig. 10) with the use of UniSorbi software for the unit SORBI-MS according to the Brunauer–Emmet–Teller (BET) theory. The estimations were made in the approximation that all the particles have the same spherical shape, the same size and they do not have pores (Table 3). Samples 2, 3, 4 were obtained from the solution with the final pH value of 8.5; while for the sample 1 pH value in a solution was equal to 9. Fig. 10

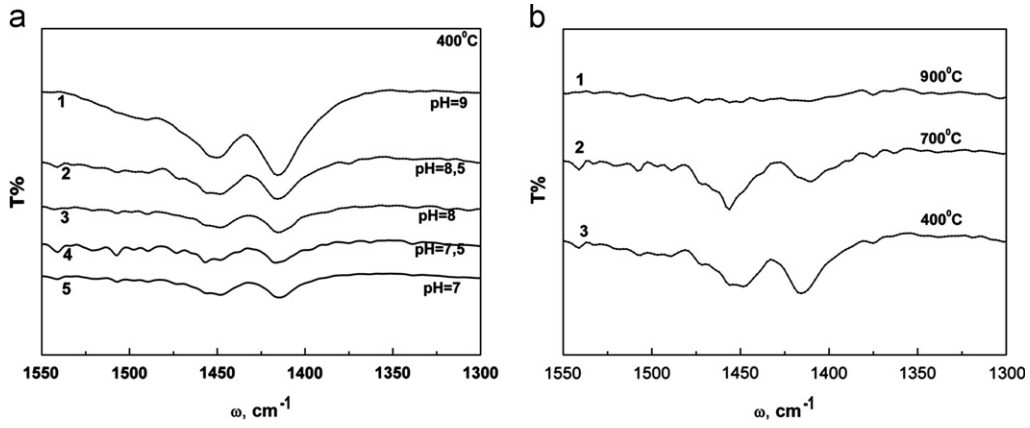

Fig. 9. IR spectra in the region 1300–1550 cm^{-1}: (a) HAP samples with different pH values, annealed at 400 °C; and (b) HAP samples with pH = 8.5 annealed at different temperatures.

provides the thermal desorption curves for nitrogen obtained from the materials synthesized under the following conditions: 1 — pH=9, 400 °C, 2 — pH=8.5 400 °C, 3 — pH=8.5 900 °C and 4 — pH=8.5 800 °C. The obtained data on thermal nitrogen desorption and the corresponding calculation results according to BET theory are presented in Table 3.

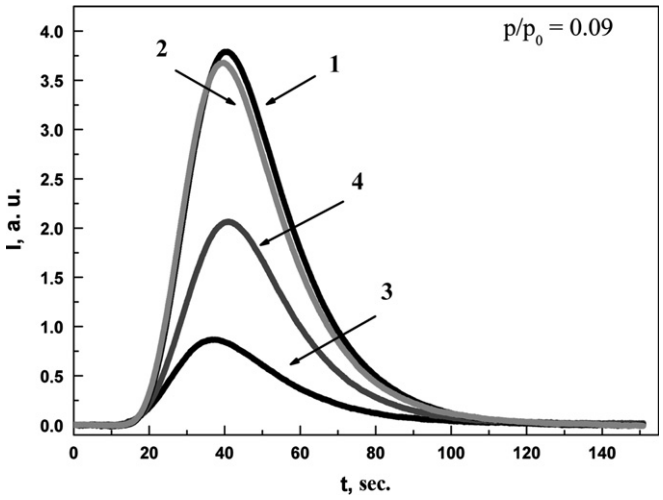

Fig. 10. Thermal desorption curves of nanocrystalline HAP powder under nitrogen partial pressure=0.09.

Specific surface calculations for HAP powders according to the thermal desorption data demonstrated that the samples 1 and 2 obtained from the solutions with different values of pH for precipitate have the same specific surface and the same size of the particles. Specific surface of the samples 3 and 4 obtained at considerably higher (900 °C) and lower (80 °C) temperatures of anneal is reduced as compared with the samples 1 and 2 that means an increase of the sizes for the particles in the powder.

Investigations of HAP powders stability to heating with the use of the SorbiPrep station for sample preparation showed that thermal exposure of the samples heated at 150 °C for 20 min does not have any effect on the specific surface of these materials.

2.5. Electron microscopy

Scanning electron microscopy was applied to study the synthesized materials morphology and to estimate the particle sizes of the samples before and after anneal. SEM images for unannealed and annealed samples of polycrystalline and synthesized hydroxyapatite are presented in Fig. 11.

Table 3
Calculations connected with thermal desorption.

	pH=9 (1) 400 °C	pH=8.5 (2) 400 °C	pH=8.5 (3) 900 °C	pH=8.5 (4) 80 °C
S sp., m^2/g (BET)	55.4 ± 0,9	55.7 ± 1.1	16.8 ± 1,2	40.2 ± 1,0
Particle size, nm ($\rho \approx 2.6$ g/cm^3)	50	50	138	60

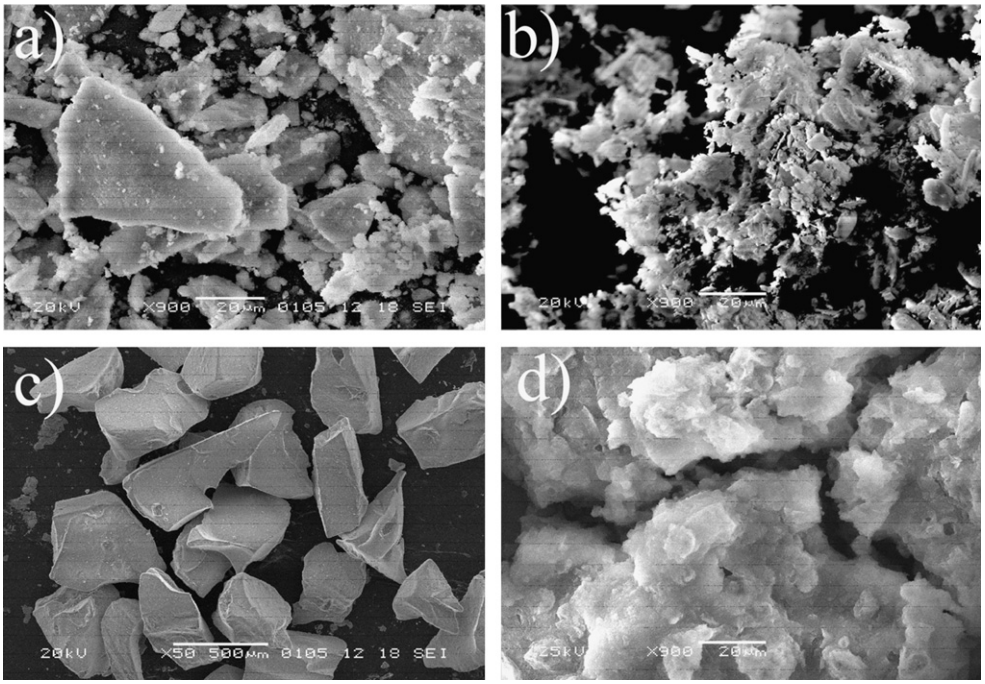

Fig. 11. SEM image of polycrystalline and synthesized HAP (a and b) — annealed at 400 °C, (c and d) — annealed at 900 °C.

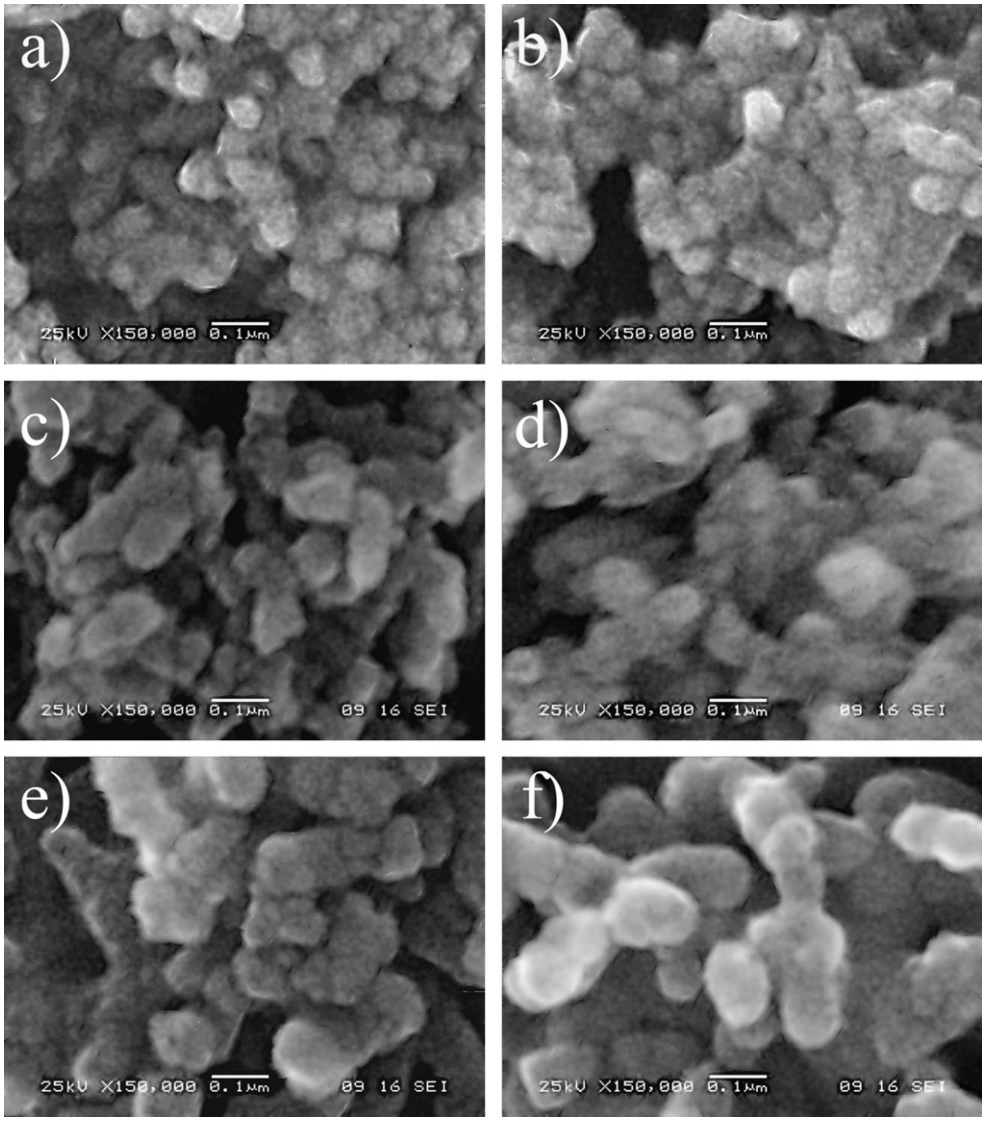

Fig. 12. SEM 150.000 of two synthesized samples annealed at 400 °C — (a and b), 700 °C — (c and d) and 900 °C — (f and g).

SEM data demonstrate that the average size of HAP particles conglomerates in the synthesized samples that were not subjected to anneal is about 5 μm (Fig. 11b) while for polycrystalline sample the average size of the particles is 20–30 μm (Fig. 11a). The images of annealed materials (Fig. 11c and d) show that in polycrystalline sample large particles which are 400 μm in size have valuable faceting (Fig. 11c).

Nanocrystals in the synthesized HAP (Fig. 11d) agglomerate after anneal forming more large particles of an arbitrary shape. The study of the synthesized materials morphology at 150000x magnification showed that the samples have a homogeneous structure (Fig. 12a and b).

Results of SEM for the samples annealed at 400 °C (a and b), 700 °C (c and d) и 900 °C (f and g) presented in Fig. 12 show that an observable agglomeration of the HAP particles proceeds at 700 °C — (Fig. 12 c and d) with formation of globules about 100 nm in size. Under further increase of temperature up to 900 °C (Fig. 12f and g) the particles reach the size of more than 150 nm.

Table 4
Elemental composition (atom%) of HAP samples synthesized with different pH, annealed at 400°C.

pH	9	8.5	8	7.5	7.05
Ca	37.64	29.74	27.57	26.74	33.03
P	15.28	16.34	14.84	15.11	17.26
O	35.67	47.37	50.17	49.72	41.96
C	10.81	6.22	7.01	8.13	7.48
Mg	0.2	0.32	0.42	0.31	0.27
Ca/P	2.16	1.82	1.85	1.77	1.71

By means of the energy-dispersion attachment Inca-250 to the electron microscope we conducted the elemental analysis of the HAP samples. The MA results allowed to determine that the elaborated technique of HAP synthesis provides hydroxyapatite samples with the different predetermined ratio

of calcium and phosphorus (Ca/P) in the material (Table 4). pH values measured in the reaction demonstrated that if pH value in HAP solution was reduced then Ca/P ratio decreased as well and it approached to the stoichiometric value of 1.67.

3. Conclusion

Investigation results obtained by means of X-ray diffraction and IR-spectroscopy show that the synthesized materials are single-phase and prove to be hydroxyapatite. Comparison of HAP synthesized with the use of eggshell and microcrystalline sample of hydroxyapatite obtained by the standard technology revealed considerable broadening of the diffraction lines of the former samples. Scherer formula based calculations demonstrate that the synthesized HAP powder granules consist of nanocrystals with the average size of $\sim$30 nm.

Temperature anneal of the samples obtained at different pH values of the solution with precipitate demonstrated that HAP powders synthesized from the solutions with the final pH value pH=7, 7.5 are characterized by less temperature stability since in these samples at 700 °C there appear diffraction peaks of the second phase — whitlockite. In the samples of HAP obtained for pH=8, 8.5 and 9 the second phase appears only at 900 °C.

IR spectroscopy gave an opportunity to detect carbonate ions impurity in nanocrystalline hydroxyapatite obtained with the use of eggshell as a source of calcium.

Comparison of all methods of analysis confirmed that with an increase of the temperature of anneal not only was a change of the phase composition observed but also an increase of the crystal sizes in HAP powder.

Thermal nitrogen desorption and scanning electron microscopy show that under annealing temperature increase a considerable agglomeration of the particles occurs as well as an increase of their sizes from $\sim$30 to $\sim$150 nm.

The results of microanalysis and measurements of pH during precipitation processes point out that with a decrease of pH in the solution containing HAP Ca/P ratio is also reduced from 2.1 to 1.7 thus approaching to the stoichiometric one; however, it does not promote an increase of temperature stability for these samples.

Acknowledgments

This work is based upon the research supported by the Foundation for Assistance to Small Innovative Enterprises in Science and Technology "U.M.N.I.K."

References

[1] T. Matsumoto, K. Tamine, R. Kagawa, Y. Hamada, M. Okazaki, J. Takahashi, Different behavior of implanted hydroxyapatite depending on morphology, size and crystallinity, Ceramic Society of Japan 114 (2006) 760–762.

[2] Melvin J. Glimcher, Molecular biology of mineralized tissues with particular reference to bone, Reviews of Modern Physics 31(2), 1959, 359–420.

[3] Toshiro Sakae, Variations in dental enamel crystallites and microstructure, Journal Oral Science 48 (2) (2006) 85–93.

[4] K.J. Lilley, U. Gbureck, A.J. Wright, D.F. Farrar, J.E. Barralet, Cement from nanocrystalline hydroxyapatite: effect of calcium phosphate ratio, Journal of Materials Science: Materials in Medicine 16 (2005) 1185–1190.

[5] S.N. Danilchenko, Structure and properties of calcium apatites in terms of biomineralogy and biomaterials technology, Vistn. Sumy Derg. Univ, Russia, 2, 2007, pp. 33–59.

[6] R. Murugan, S. Ramakrishna, Development of cell-responsive nanophase hydroxyapatite for tissue engineering, American Journal of Biochemistry and Biotechnology T3 (3) (2007) 118–124.

[7] C. Rey, C. Combes, C. Drouet, H. Sfihi, A. Barroug, Physico–chemical properties of nanocrystalline apatites: implications for biominerals and biomaterials, Material Science and Engineering 27 (2007) 198–205.

[8] M. Prodana, D. Bojin, D Ionita, Effect of hydroxyapatite on interface properties for alloy/biofluid, U.P.B. Scientific Bulletin 71 (4) (2009) 1454–2331.

[9] D. Eichert, H. Sfihi, M. Banu, S. Cazalbou, C. Combes, C. Rey, Surface structure of nanocrystalline apatites for bioceramics and coatings, Advances in Science and Technology 41 (2002) 14–18.

[10] J.M. Cao, J. Feng, S.G. Deng, X. Chang, J. Wang, J.S. Liu, P. Lu, H.X. Lu, M.B. Zheng, Zhang, J. Tao, Microwave-assisted solid-state synthesis of hydroxyapatitenanorods at room temperature, Journal of Materials Science 40 (2005) 6311–6313.

[11] M.V. Chaikina, V.F. Pichugin, M.A. Surmeneva, R.A. Surmenev, Mechanochemical synthesis of isomorphous varieties of apatite as functional materials, Chemistry for Sustainable Development T17 (2009) 513–520.

[12] C. Guzmán Vazquez, C. Pina Barba, N Munguúa, Stoichiometric hydroxyapatite obtained by precipitation and sol gel processes, Revista Mexicana de Fisica 51 (3) (2005) 284–293.

[13] I. Sopyan, R. Singh, M Hamdi, Synthesis of hydroxyapatite powder using sol–gel technique and its conversation to dense and porous bodies, Indian Journal of Chemistry 47A (2008) 1626–1631.

[14] X. Du, Y. Chu, S. Xing, L Dong, Hydrothermal synthesis of calcium hydroxyapatite nanorods in the presence of PVP, Journal of Materials Science 44 (2009) 6273–6279.

[15] N.D. Luong, J.-D. Nam, Synthesis of hydroxyapatite and application in bone and dental regeneration in human body, Sungkyunkwan University, 2001, p. 4.

[16] T.V. Thamaraiselvi, K. Prabakaran, S. Rajeswari, Synthesis of Hydroxyapatite that Mimic Bone Mineralogy, Trends in Biomaterials and Artificial Organs 19 (2) (2006) 81–83.

[17] J. Gomez-Morales, J. Torrent-Burgues, T. Boix, J. Fraile, R. Rodrigues-Clemente, Precipitation of Stoichiometric Hydroxyapatite by a Continuous Method, Crystal Research and Technology 36 (1) (2001) 15–26.

[18] K. Benzerara, T.H. Yoon, T. Tyliszczak, B. Constantz, A.M. Spormann, G.E. Brown, Scanning transmission X-ray microscopy study of microbial calcification, Journal of Geobiology N2 (2004) 249–259.

[19] H. Eslami, M. Solati-Hashjin, M Tahriri, H. Eslami, Synthesis and characterization of hydroxyapatite nanocrystals via chemical precipitation technique, Iranian Journal of Pharmaceutical Sciences 4 (N2) (2008) 27–134.

[20] D.W. Kim, I.-S. Cho, J.Y. Kim, H.L. Jang, G.S. Han, H.-S. Ryu, H. Shin, H.S. Jung, H. Kim, K.S. Hong, Simple large-scale synthesis of hydroxyapatite nanoparticles: in situ observation of crystallization process, Langmuir 26 (1) (2009) 384–388.

[21] J. Liao, L. Zhang, Y. Zuo, H. Wang, J. Li, Q. Zou, Y. Li, Development of nanohydroxyapatite/polycarbonate composite for bone repair, Biomaterials Applications N4 (2009) 31–43.

[22] K. Deepak, R.D. Pattanayak, R.C. Prasad, B.T. Rao, M. Rama, Synthesis and sintered properties evaluation of calcium phosphate ceramics, Materials Science and Engineering 27 (4) (2007) 684–690.

[23] A. Siddharthan, S.K. Seshadri, T.S. Sampath Kumar, Rapid synthesis of calcium deficient hydroxyapatite nanoparticles by microwave

irradiation, Trends in Biomaterials and Artificial Organs 18 (2) (2005) 110–113.
[24] K. Prabakaran, A. Balamurugan, S. Rajeswari, Development of calcium phosphate based apatite from hen's eggshell, Bulletin of Materials Science 28 (2) (2005) 115–119.
[25] M.F. Raihana, I. Sopyan, M. Hamdi, D.S. Ramesh, Novel chemical conversion of eggshell to hydroxyapatite powder, Biomed N21 (2008) 333–336.
[26] S.J. Gadaleta, E.P. Paschalis, F. Betts, R. Mendelsohn, A.L. Boskey, Fourier transform infrared spectroscopy of the solution-mediated conversion of amorphous calcium phosphate to hydroxyapatite: new correlations between X-ray diffraction and infrared data, Calcified Tissue International N58 (1996) 9–16.
[27] N. Pleshko, A. Boskey, R. Mendelsohn, Novel infrared spectroscopic method for the determination of crystallinity of hydroxyapatite minerals, Biophysical Journal 60 (1991) 786–793.
[28] S. Ramesh, C.Y. Tanb, M. Hamdib, I. Sopyanc, W.D. Tengd, The influence of Ca/P ratio on the properties of hydroxyapatite bioceramics. S. Ramesh (Ed.), in: Proceedings of the International Conference on Smart Materials and Nanotechnology in Engineering, 6423(64233A), 2007, pp. 1–6.
[29] A.P. Karnaukhov, Adsorption. Texture of disperse and popous materials, Novosibirsk, Nauka, 1999, 470 p (in Russian).
[30] JCPDS–ICDD, Card No. 9-432, 1995.
[31] A.P. Shpak, V.L. Karbovsky, V.V. Trachevsky, Apatites, Academperiodika, Kiev, 2002, p. 414 (in Russian).
[32] O.A. Anunziata, L. Maria, M.R. Beltramone, A.R. Beltramone, Hydroxyapatite/MCM-41 and SBA-15 nano-composites. preparation, characterization and applications, Materials 2 (2009) 1508–1519.
[33] I.R. Gibson, W. Bonfield, Novel Synthesis and Characterization of an Ab-Type Carbonate-Substituted Hydroxyapatite, J Biomed Mater Res. 2002, pp. 697–707.
[34] K. Jonas, I. Vassanyi, I. Ungvari, The study of synthetic carbonate–hydroxyapatites and dental enamels by ir and derivatographic methods, Physics and Chemistry of Minerals 6 (1980) 55–60.
[35] Y. Yusufoglu, M. Akinc, Effect of pH on the carbonate incorporation into the hydroxyapatiteprepared by an oxidative decomposition of calcium–edta chelate, Journal of the American Ceramic Society 91 (1) (2008) 77–82.